ROCK FAILURE

NUMERICAL MODELING OF HYDRAULIC FRACTURE INITIATION AND DEVELOPMENT

V. V. Zubkov, V. F. Koshelev*, and A. M. Lin'kov*   UDC 622.83+539.4

Studying initiation and propagation of hydraulic fractures is carried out based on the hypersingular boundary element method.

Geomechanics, hydraulic fracture, numerical modeling

INTRODUCTION

The most effective and widely applied method for enhancing influx of a fluid (oil, gas) into a well is the hydraulic fracturing of rocks. The method is also used to alleviate burying conditions for unwanted substances (carbon dioxide, contaminants, radionuclides, etc.) and for geothermal energy extraction. Starting from a pioneer research by Zheltov and Khristianovich [1], the hydraulic fracturing has become a subject of many investigations [2–21], with the result presented in monographs [22] and reviews [23]. Theory and practice have been generalized in the studies [24] and recommendations of the International Society for Rock Geomechanics [25].

The subject of the most of theoretical studies is the simplest scheme of a rectilinear or circular crack under different interaction conditions of its edges [1, 11, 26–31]. As a rule, no consideration is given to an unsteady flow from a rock to a crack, that causes change in a stress state and leads to formation or closing of the channels. The hydraulic fracturing-induced seismic emission in a rock mass and further changes in filtration process were entirely left aside. So, we have a lot of important questions to answer as we speak about the hydraulic fracturing.

Combining the newest calculation methods and experimental and observational data available facilitates and hastens the search for the answers. To follow along this path, the authors of the present paper engaged a newly developed method of hypersingular integral equations and the respective boundary element method (BEM) for adding to the abilities of the hydraulic fracturing numerical modeling. Moreover, it becomes possible to reveal the role of scattering and indefiniteness in sizes of initial (incipient) cracks and in strength characteristics, to bring in accord different linear scales, which may vary from decimeters for a well to tens and even hundreds meters for a formed hydraulic fracture, and to ensure stable estimates of a propagating shell-like fracture in a compressive stress field.

"VNIMI" Joint-Stock Company, E-mail:zubkov@vnimi.ru, Saint Petersburg, Russia. *Institute of Problems of Machine Science, E-mail: linkov@hotmail.com, Saint Petersburg, Russia. Translated from Fiziko-Tekhnicheskie Problemy Razrabotki Poleznykh Iskopaemykh, No. 1, pp. 45-63, January-February, 2007. Original article submitted November 3, 2006.

All these problems were not discussed in the first publications on this topic [32–34] that mostly illustrated the new capacity developed as a result of the hypersingular BEM. The present authors have faced these problems when initiated the "Hydromethan" project*. This paper answers the stated questions.

Below we study a fracture initiation and propagation in a simplified statement up to the classical failure mechanics, and fluid motion in a crack and its filtration to a rock is beyond our attention. This statement is acceptable for modeling growth onset for a small crack [35] and is, thus, incapable of depicting the process in full if the crack length exceeds much a well diameter. Therefore, we withdraw from our discussion the questions on time dependence of the growing crack trajectory and which length corresponds to the growth stop.

However, the improved algorithm and obtained results facilitate changing over to the next stage, that is taking into account the fluid motion. This passage is easy to do within the framework of the scheme from [35], i.e., by adding an equation of flow in an alternating section gap and a Carter type law of leakage. This will only change pressure distribution inside the crack at the algorithm stages of following by itself the crack growth, the algorithm and the whole program unaltered. In addition, some conclusions that were drawn for the simplified scheme, will hold true for the fluid motion. For example, the conclusions on crack propagation in the direction of maximum compression, on "elliptical" displacement discontinuity distribution for a long crack and on the limiting stress intensity factor value having almost no effect on the crack growth.

The study is carried out for the plane strain conditions. Later, we assume changing over to 3-D modeling, integration of modeling unstable filtration in a crack and in rocks and involvement of seismic processes into the analysis.

CALCULATION SCHEME AND THE SOLUTION METHOD

A standard hydraulic fracturing modeling scheme is a horizontal section of a vertical well with an initial crack originating at the well boundary (Fig. 1).

Let the rock mass be homogenous and isotropic. Original stress state of the rock mass (prior to drilling the well) is described by three principal components:** $\sigma_3^0 = -\gamma H$, $\sigma_1^0 = -\lambda_1 \gamma H \equiv -\sigma_h$, $\sigma_2^0 = -\lambda_2 \gamma H \equiv -\sigma_H$, where σ_3^0 are the vertical stresses; σ_1^0 and σ_2^0 are the horizontal stresses in the direction of x_1 and x_2; γ is the average gravity of rocks; H is the hydraulic fracturing making depth; λ_1 and λ_2 are the lateral thrust coefficients in the direction of x_1 and x_2, respectively.

The x_3 axis is vertically upward, the axes x_1 and x_2 are in the horizontal plane and coincide with the directions of σ_h and σ_H, respectively; the angle φ determines the initial crack orientation relative to the direction of the minimal horizontal stress σ_h (for the definiteness, it is assumed that $\sigma_H \geq \sigma_h$). We suppose that upon fluid injection, the well contour and the boundaries are applied with a uniform pressure *p*. After reaching a limit $p = p_b$, the hydraulic fracturing begins. The hydraulic fracture growth direction depends on stresses in the vicinity of the crack tip; the stresses, in their turn, depend on the combination of the original fields, fluid pressure and current geometry of the hydraulic fracture. Estimating possible propagation of the fracturing and its direction needs solving a boundary-value problem, i.e., finding the mentioned stresses for the current geometry of the hydraulic fracturing and under the assigned boundary conditions.

**The compressive stresses are negative.
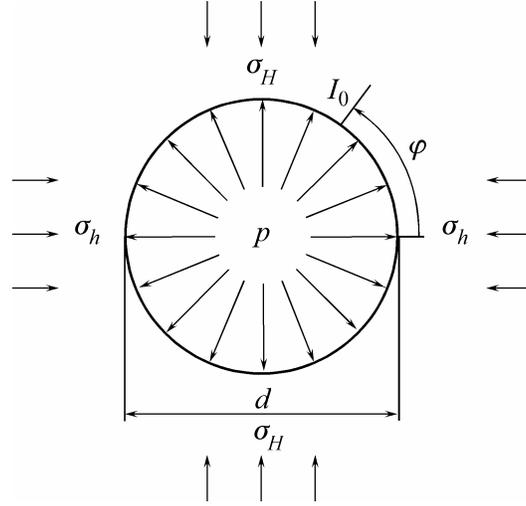
Fig. 1. Calculation scheme for modeling a hydraulic fracturing process: horizontal section of a well and an initial crack

Geometry of the calculation scheme is complex, thus, we need numerical modeling methods for the solution. It seems the most natural to use the boundary element method based on the boundary integral equations (BIE) of the plane problem of the elasticity theory. The BEM, unlike FEM, for instance, assumes digitizing only the considered domain boundary, in our case, this is the well and crack section contour. The result is a large saving of computational resources. The used BEM variant is based on the complex hypersingular equations whose advantages as compared with the method developed in [36] and found a systematic application in problems of geomechanics [26 – 29], are described in detail in [37]. Along with the well-known analytical advantages, the equations in question allow simple and correct accounting for the crack coming out on the domain contour, branching of cracks and complex contact interactions. This fact is important for calculation schemes that include geological disturbances near the hydraulic fracturing propagation front and inhomogenous blocks.

A complex hypersingular equation has the form:

$$\frac{1}{2\pi i}\int_S\left\{\frac{2\Delta u}{(\tau-t)^2}d\tau-\Delta u\frac{\partial}{\partial t}dk_1-\Delta\bar{u}\frac{\partial}{\partial t}dk_2+(2a_1-a_3)\frac{\sigma d\tau}{\tau-t}\right\}+$$

$$+\frac{1}{2\pi i}\int_S\left\{(a_1-a_3)\sigma\frac{\partial k_1}{\partial t}d\tau+a_1\bar{\sigma}\frac{\partial k_2}{\partial t}d\bar{\tau}\right\}=\frac{a_2}{2}\sigma(t)+S^\infty. \tag{1}$$

In (1) integration is performed by a common boundary S of the domain including a fracture or a family of fractures, together with a contour of the well where from the hydraulic fracturing propagates, and a system of natural disturbances and boundaries of blocks. Points at S are determined by complex variables t ("observation" point) and τ (integration variable); stroke above a symbol means a complex conjunction. The main kernels in (1) are as follows: $k_1(\tau,t)=\ln\dfrac{\tau-t}{\bar{\tau}-\bar{t}}$, $k_2(\tau,t)=\dfrac{\tau-t}{\bar{\tau}-\bar{t}}$. Real constants a_j ($j=1,2,3$) depend on Young's moduli and Poisson's ratios the blocks have on different sides of S; S^∞ is a linear function of stresses in an intact rock mass [37].

42

At different sections of the boundary, either the forces $\sigma(t)$, or the displacement discontinuities $\Delta u(t)$, or the relation to connect these values are assigned. In particular, the assigned forces on the surface of the hydraulic fracturing depend on the fluid pressure. In the general problem statement, this pressure is unknown beforehand and is found by solving a joint problem on the fluid flow and rock deformation. The system of equations should also involve relations for fluid filtration in joints and inside the coal seam if the hydraulic fracturing crosses it. The fluid pressure in the simplified problem statement may be used as an assigned value, based on data about a breakdown pressure and typical dependences of the pressure on the injected liquid volume or injection duration.

We solve (1) by the complex BEM founded upon a discrete representation of the boundary as a set of elements: rectilinear segments and arcs of circles. Unknown functions are approximated inside each of the elements by a second-order, power (for rectilinear elements) or trigonometric (for the elements along the arcs of circles) polynomial. Special final elements are for tips of cracks. The displacement discontinuities are represented on the final elements by the product of a second-order polynomial and a square root of a distance to the tip. This kind of approximation of the usual and final elements ensures high accuracy and reliability of the results for the stress concentration area near the hydraulic fracture tip.

While the hydraulic fracturing is propagating, the boundary S conforms to its current geometry. It is necessary to know the propagation direction in each step of the process, wherefore a sequence of problems is solved for small increments directed at different angles towards a tangent at the final point of the current shape. For this purpose, the studies [38, 39] present the specially developed algorithms for highly accurate and stable calculation. The algorithms help detecting the fracture trajectory by itself. The present authors have modified this procedure for the problem on the hydraulic fracturing with allowance for the problem features discussed below.

To date, by the modeling method, it is possible to determine the onset conditions for a hydraulic fracturing and to plot reliably its trajectory.

BREAKDOWN PRESSURE

The key parameters for a hydraulic fracturing realization in practice are a breakdown pressure p_b and a shut-in pressure p_s [25] that correspond to the fracturing growth start and to the large propagation of the fracture, respectively.

From the viewpoint of mechanics, p_b is a pressure needed for initiating development of an initial crack. This pressure must be high enough to overcome compressive forces immediately at the well contour, where, as is known, there is a high stress concentration as compared with the zone remote from the well. The fracture is growing, and the well almost looses its influence when the distance between the fracture and the well is more than three – four well diameters, and now it is only necessary to overcome stresses of the intact rock mass.

The procedure described in the previous section allows computing both the breakdown and shut-in pressures. We can do this for the prime pattern with involving an isolated well and a single, propagating from it fracturing for a more general scheme with any, practically reasonable, set of wells and fractures. In the latter case, the breakdown pressure corresponds to the onset of the most "dangerous" fracture growth.

However, the prime pattern is of the most importance for the hydraulic fracturing mechanics, as it yields estimates of technological parameters and assists in analyzing parameters and techniques essential for numerical modeling. Below we cite some calculation data for the breakdown pressure,

obtained with no information about this values available beforehand. The geometry characteristics and initial stress state are assigned, and the problem with a gradually rising pressure of liquid is solved by BEM. A start pressure is taken as $0.5\sigma_h$ and it then gradually rises with a small step $0.05\sigma_h$; this step governs the actual calculation accuracy for the breakdown pressure that corresponds to the satisfied strength condition in the theory of cracks:

$$K_I = K_{IC}, \tag{2}$$

where K_I is a stress intensity factor (SIF) by an opening fracture mode dependent on the assigned forces and the problem geometry; K_{IC} is the SIF limit. Table 1 gives the values of the breakdown pressure p_b, rated by σ_h and fitting a fixed dimensionless parameter $\mu = \dfrac{K_{IC}}{\sigma_h\sqrt{d/2}} = 0.1$ and an initial crack length l_0 to a well diameter d ratio of 0.1. These relations are quite standard for the hydraulic fracturing conditions, in particular, $\mu = 0.1$ when $\sigma_h = 20$ MPa, $d = 0.14$ m and $K_{IC} = 0.53$ MPa·m$^{1/2}$.

It is obvious in Table 1 that p_b is close to the intact rock mass stress σ_h if the initial fracture orientation is at the angle φ more than 45°. The breakdown pressure only exceeds σ_h more than by 10 % when the initial fracture orientation is unfavorable, at an angle less than 45° toward the minimum stress direction. In exceptional cases, when there are no favorably oriented initial fractures near the well and the initial stress components ratio reaches 2, the breakdown pressure can be twice as high as the stress σ_h.

Proceeding from simple theoretical considerations and condition (2), we estimate p_b in order to simplify modeling of an onset stage of the hydraulic fracturing, since a serial search of the growing pressure values adds to the computational period. Considerations of the dimensions implies that in the problem on a fracture with a length l_0, growing from contour of a hole with a diameter d, when $l_0/d \ll 1$, SIF can be presented as [40]:

$$K_I = \alpha\sqrt{\pi l_0}(2p + \sigma), \tag{3}$$

where σ is a nominal (regardless fracture) circumferencial stress at the well contour where the fracture is; α is a factor dependent on l_0/d. In extreme case, when $l_0/d \to 0$, we have $\alpha = 1.12$, which corresponds to a fracture perpendicular to the half-plane boundary [41]. In this case, (3) assumes the form:

$$K_I = 1.12\sqrt{\pi l_0}(2p + \sigma). \tag{4}$$

For a hydrostatic initial stress field in a rock mass ($\sigma_H = \sigma_h = q$), $\sigma = -2q$. When $\sigma_H \neq \sigma_h$, we have:

$$\sigma = -\sigma_h[3 - \delta + 4(\delta - 1)\cos^2\varphi], \tag{5}$$

where $\delta = \sigma_H/\sigma_h$.

TABLE 1. The Rated Breakdown Pressures p_b/σ_h Found by BEM for $\mu = 0.1$ and $l_0/d = 0.1$)

φ, deg	0	30	45	60	90
$\sigma_H/\sigma_h = 2.0$	2.35	1.50	1.15	1.05	0.85
$\sigma_H/\sigma_h = 1.2$	1.35	1.25	1.15	1.10	1.05

TABLE 2. The Rated Breakdown Pressures p_b/σ_h for $\alpha=1.12$

φ, deg	0	30	45	60	90
$\sigma_H/\sigma_h=2.0$	2.56	2.06	1.56	1.06	0.56
$\sigma_H/\sigma_h=1.2$	1.36	1.26	1.16	1.06	0.96

Using relations (2) and (5), find the breakdown pressure:

$$\frac{p_b}{\sigma_h} = \frac{3-\delta}{2} + 2(\delta-1)\cos^2\varphi + \frac{K_{IC}}{2\alpha\sqrt{\pi l_0}\sigma_h}. \tag{6}$$

Table 2 gives the breakdown pressures calculated from (6) for $\alpha=1.12$.

Comparing Table 1 and Table 2 data shows that when σ_H/σ_h is close to one, an analytical estimate of the breakdown pressure is rather close to the numerical modeling results for any angle of the initial fracture. When the stress components differ much ($\sigma_H/\sigma_h=2.0$), the analytical estimate varies greatly from the numerical value obtained for $l_0/d=0.1$, especially when $\varphi=45°$ and 90°. The main reason of error of the simplified theoretical estimate is that relation (5) yields the circumferencial stresses strictly at the contour, while the fracture tip is markedly apart from it and is in the nominal stress field somewhat less than given by (5).

To make the simplified estimates more accurate, use the known, tabular stress intensity factors for the finite length cracks coming from a circular hole contour [41]. These values relate to the cases when forces are assigned at infinity and act along a normal to the crack or in parallel to it. The prime hydraulic fracturing pattern for a crack going along the action direction of any of the principal stress σ_H or σ_h is reduced to such problem by the field superposition method: assigning of the equivalent stresses $\sigma_1^\infty = p-\sigma_h$, $\sigma_2^\infty = p-\sigma_H$ at infinity is only necessary. When the fracture is out of any of the said directions, the equivalent field contains non-zero components of shear stresses; for such angles there are unfortunately no tabulated SIF in [41]. The comparison data for the thus obtained estimates and the BEM calculation results for the cases described in the handbook [41] ($\varphi=0°$ and 90°) is presented in Table 3.

The results seem to agree quite satisfactorily. Deviation is somehow due to discreteness of the pressure increment steps ($0.05\sigma_h$) when meeting limiting condition (2).

The above cited simple estimates are interesting from two points of view. First, they empower inverse calculations when the breakdown pressure is established experimentally and the more or less precise data is available on enclosing rock properties, original stress state and/or initial fracture orientation and size. In this case, we can find missing characteristics, for instance, an intact rock mass stress by using the pre-existing fracture method [25]. Second, it is possible to perform an analysis of sensitivity to the change in parameters, which are quite uncertain in the hydraulic fracturing problems, for example, the angle and initial length of the hydraulic fracture.

TABLE 3. The Rated Breakdown Pressures p_b/σ_h

φ, deg		0	90
$\sigma_H/\sigma_h=2.0$	BEM	2.35	0.85
	Data from [34]	2.48	0.70
$\sigma_H/\sigma_h=1.2$	BEM	1.35	1.05
	Data from [34]	1.37	1.01

Now we illustrate simplification of the solution for the problem on the breakdown pressure for conditions of relatively large depths. In the above-discussed calculation example using (6), the last number on the right-hand side was negligible as compared with the rest ones. It is important to know how wide is the range of such conditions, as these are the cases when we can do without assigning K_{IC} and initial length of fracture. Given anomalously high δ are taken away, to answer the question needs the following condition to be met:

$$\frac{K_{IC}}{2\alpha\sqrt{\pi l_0}\,\sigma_h} \ll 1. \qquad (7)$$

In principle, it governs the estimate precision for the breakdown pressure with no data on initial length and SIF. We take $K_{IC} = (0.5 \div 1)$ MPa·m$^{1/2}$ for sedimentary rocks [42, 43]. In this case, for example, for an initial fracture 1 cm in length, conditions (7) is met when $2\alpha\sigma_h \gg 2.8 \div 5.6$. For $\alpha = 1.12$, $\sigma_h = \gamma H$, $\gamma = 25$ kN/m^3, we have that $H \gg (50 \div 100)$ m. For our example, even for $H = 500$ m, the error of neglecting the SIF-containing member is small. In fact, having taken $K_{IC} = 1$ MPa·m$^{1/2}$, we find from (6) that $p_b/\sigma_h = 1.50 + 0.20 = 1.70$ for $\delta = 2$ and $\varphi = 45°$. Whence it follows that neglecting the last number equaling 0.20 in (6) allows less than 12 % error in the breakdown pressure determination.

As the hydraulic fracture is growing and its tip is moving away from the well, relationships of finding the stress intensity factor acquires a more general form as compared to (3):

$$K_I = \sqrt{\pi l}\,f(p - \sigma_H, p - \sigma_h), \qquad (8)$$

where l is the current length of trajectory; f is a function dependent on the hydraulic fracture shape and distance from the well and is found numerically when modeling the hydraulic fracturing by BEM. When the trajectory has largely developed and its rectilinear section prevails over the initial curvilinear part, we can assume $f = (p - \sigma_h)/\sqrt{2}$, i.e. $K_I = \sqrt{\pi l/2}(p - \sigma_h)$, where l is the length of the fracture added with the well diameter, as apart from the well its influence is almost equivalent to the influence of the respective linear fracture.

Back on estimating effect of the last number in (6), it is possible to state that its role, at a largely grown length, is much less than at the start of the hydraulic fracture propagation. For the ten- and hundredfold grown hydraulic fracture, the nominal stresses to be overcome by the fluid pressure are governed by the intact rock mass stresses only (subject to the restriction of no effect of the geological disturbances). At a distance from the well, the hydraulic fracture orients in perpendicular to the action of σ_h. And this is σ_h that acts as the nominal stresses and is to be overcome by the working pressure. This conclusion is completely supported by the below calculations for the fracture trajectory after reaching the breakdown pressure.

The definition of the breakdown pressure, which we have considered earlier, needs an adjustment for the conditions when the intact rock mass stress components differ greatly, that is $\sigma_H/\sigma_h > 2$. At the same time, as follows from (5), the state when $|\sigma| < \sigma_h$ is also possible, for example, when $\varphi = 90°$. This means that when the fracture starts propagating in this direction or close to it, the fracturing front should transfer from the zone with a relatively low compression to a stronger compression zone: at a distance from the well $\sigma \approx \sigma_h$. Therefore the fracture growth initiation pressure may be somewhat lower than the pressure to overcome the maximum compression zone, and it is expedient to assume the latter value as the breakdown pressure and differentiate it from the hydraulic fracture initiation pressure.

One more remark is to be made on possibility of interpreting (2) and (3) from the viewpoint of concepts that do not use the fracture mechanics. Let the limiting condition be:

$$2p + \sigma = \frac{K_{IC}}{\alpha\sqrt{\pi l_0}}.$$ (9)

The right-hand side of (9) is a limit T to be reached or overcome to initiate a hydraulic fracture. The left-hand side is a total force that positive (tensile) when the pressure is sufficiently high. So far, (9) expresses a tensile strength condition if we interpret T as a relevant limit. Actually this meaning is imparted on the limiting condition and breakdown pressure in the known review [23]. Given (5) involves $\varphi = 90°$, then $\sigma = -3\sigma_h + \sigma_H$. In this case, (9) yields a relationship for determining p_b: $2p_b + 3\sigma_h - \sigma_H = T$ that differs from the breakdown pressure equation from the mentioned review by coefficient 2 attached to p_b. This coefficient reflects a combined effect of the pressures on the well contour and the fracture edges. Useful for estimating the breakdown pressure, this interpretation, however, keeps out of determining the fracture trajectory and, thus, the equality of the intact rock mass stress minimum and the working pressure ($|\sigma_h| = p_s$) in [23] is postulated a priori and is not calculated (as below) as a result of the fracture coming out onto a rectilinear trajectory when $K_I \gg K_{IC}$.

POST-INITIATION FRACTURE GROWTH MODELING

Upon reaching the breakdown pressure, the fracture propagation direction, as a rule, deviates from the initial fracture orientation and tends to the action direction of the highest principal stresses in the intact rock mass. An appropriate fluid injection mode sustains the well pressure sufficiently high to satisfy fracture growth condition (10) until a gradually rising filtration resistance or deficient injection rate leads to a drop of the pressure and break of the fracture development:

$$K_I \geq K_{IC}.$$ (10)

Usually the fracture has time to grow by several tens and even hundreds meters by this moment. In mathematical description, the hydraulic fracture stops growing when condition (10) is violated.

The Fracture Trajectory Calculation Method. In the general case, a hydraulic fracture is an unknown surface in space. In the plane problem, a fracture trajectory, far and by, is a curve in the horizontal section of the well. Solving practical tasks, such as rational injection regime specification, proppant application and further operation of the well requires numerical modeling of the fracture trajectory and condition (10) is not enough for this. A supplementary condition to control the fracture growth direction every moment of its propagation is necessary.

We use a trajectory plotting approach related to the abilities of the above-described numerical modeling of stress state in the framework of plane strain. A criterion of determining the fracture development direction bases on classical concepts that are valid when an opening fracture mode prevails. In this case, as is known, a number of physically feasible criteria become equivalent for trajectories with a continuously alternating tangent vector [44]: the maximum SIF K_I, maximum energy release rate, energy density index time invariance, maximal shear stresses. Any of them is expressed mathematically as the equality:

$$K_{II} = 0.$$ (11)

In [38] a special iteration method is developed for auto-tracing trajectories based on condition (1). The method involves final elements along arcs of circles, which allows a smooth conjunction of the elements. Figure 2 gives an explanation of the sense of the method.
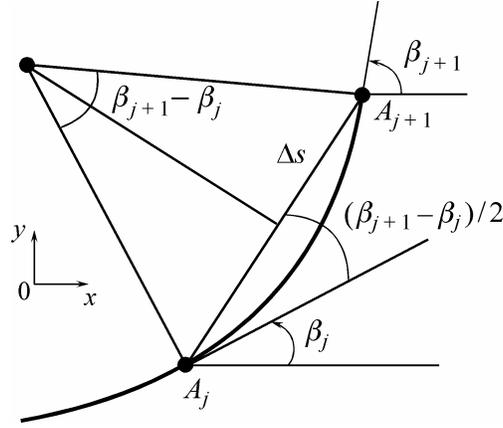
Fig. 2. Calculation scheme for the fracture trajectory

A complex coordinate z_{j+1} in a new fracture end position A_{j+1}, at a step $j+1$ is calculated in terms of z_j from the formula:

$$z_{j+1} = z_j + \Delta s \exp(i(\beta_j + \beta_{j+1})/2),\qquad(12)$$

where z_j and z_{j+1} are the complex coordinates of the points A_j and A_{j+1}, respectively; Δs is a length of the A_j-to-A_{j+1} chord; β_j and β_{j+1} are the angles formed by tangents to the x axis of the global coordinate system at these points. The angle β_{j+1} varies and is selected so that condition (11) is satisfied for the fracture tip in the new position.

Auto-collecting β_{j+1} follows the iteration procedure below:

$$\beta_{j+1}^m = \beta_{j+1}^{m-1} + g\theta_{j+1}^{m\text{-}1},\qquad(13)$$

$$\theta_{j+1}^{m-1} = 2\mathrm{arctg}\{[\,1 - \mathrm{sign}(K_I^{m-1})\,\sqrt{1 + 8(K_{II}^{m-1}/K_I^{m-1})^2}\,]/(4K_{II}^{m-1}/K_I^{m-1})\}\,,\qquad(14)$$

where $m, j = 1, 2, \ldots$; $\beta_{j+1}^0 = \beta_j + \beta^0$, β_j is an angle value obtained in the previous, jth incremental step for the fracture; β_0 is the preassigned initial deviation; m is the iteration number; g is a relaxation parameter for iteration convergence and its values are selected automatically in a range from 0.5 to 1. Iteration stops upon reaching the preset accuracy of β_{j+1} (usually 0.5°). The iteration procedure and its parameters selection is described in detail in [38, 45] where also is shown, using some examples, that the iteration results are more precise as compared with the earlier applied methods [38].

It follows from (13), (14) that each step search for the trajectory continuation is limited by a regular, single application of formula (14) for a likely angle of the tangent at the fracture tip. This search is a consistent enumeration of some increments of the fracture in various directions, with gradual reaching the fracture tip position such that condition (11) is met within the preset accuracy. As a rule, this process needs 5 iterations. So far, unlike the previous simplest algorithms, each fracture incremental step corresponds to a series of solutions of the hypersingular integral equations ($m = 1, 2, \ldots$) for virtual shapes of the fracture.

48

The Trajectory Search Stability Provision. The application of iterations $(12)-(14)$ to the problems on the hydraulic fracture propagation has demonstrated that, differently to the problems from [38, 39, 45–47], this algorithm is, however, unstable sometimes. A comprehensive study revealed that the instability arises when the intensity factor K_I passes the zero value, for instance, under start of the initial fracture oriented in perpendicular to the maximal compression direction. In this case, when negative K_I are modulo small, formula (14) yields an angle that equals $2\mathrm{arctg}(1/\sqrt{2}) = 70.53°$ for $K_{II} < 0$ or $-70.53°$ for $K_{II} > 0$, and further search provides no convergence. The situation worsens if K_{II} is modulo small as well. Besides, at small K_{II} meeting the equality condition in (11), the values of θ_{j+1}^{m-1} begin oscillating sometimes: the values of θ_{j+1}^{m-1} on the next 2 iteration become equal but opposite in sign, close to zero, but higher than the preset accuracy of meeting (11), which generates the algorithm circling. To overcome these difficulties, the authors have modified algorithm $(12)-(14)$ by two complements introduced. First, when $K_I < 0$ and $(K_I/K_{II})^2 < 0.1$, the right-hand side of (14) is assumed to be zero. Second, a sum of the values of θ_{j+1}^{m-1} on next 2 iteration must be checked: if the sum is less than 0.01, the angle is put to zero. These complements release the iteration from any random walks and oscillations.

The Boundary Element Mesh Modification. Mostly, in practice, a hydraulic fracturing is a means of enhancing oil and gas recovery, and it serves its purpose if propagates for tens or hundreds meters. Bearing in mind that a well diameter is $10-15$ cm and initial defects are of the order of the first centimeters in length, we realize an extent of the geometrical scale difference of the hydraulic fracture modeling problem.

A key point of the modeling initial stage of a fracture growth is the contour of the well and initial fracture. Provision of admissible calculation accuracy needs paying peculiar attention to digitization of the boundary in the zone near the well mouth where the displacement gradients are extremely high. While the hydraulic fracture front is moving away from the well, this zone becomes of lesser effect. It is possible to replace a detail displacement distribution by average values without loss of accuracy, i.e., a set of small boundary elements near the mouth is replaceable with one or two larger elements and the well is assumed as an initial part of the fracture. Such an elemental modification for calculating extended fractures allows a shorter computational period and saves from the computational instability typical for the cases when there are many boundary elements and they have sharply differing sizes.

The fracture trajectory modeling scheme was added with a block of the boundary element mesh modification with the fracture length increased up to a certain preset value. To illustrate the accuracy of this technique, consider an example when the fracture length is tenfold as the well diameter (for longer fractures, the boundary element mesh modification accuracy is much higher).

Figure 3 shows a trajectory of the hydraulic fracture propagation at the stresses at infinity as σ_H and σ_h ($\sigma_H/\sigma_h = 1.2$) and internal pressure in the well and in the fracture as $p = 1.35\sigma_h$. The trajectory contains a rectilinear section, that runs in parallel to the action of σ_h and is a continuation of the initial fracture, and an arc of a circle where a smooth pass to a σ_H action-parallel line takes place. The latter line is the third, rectilinear section of the fracture.
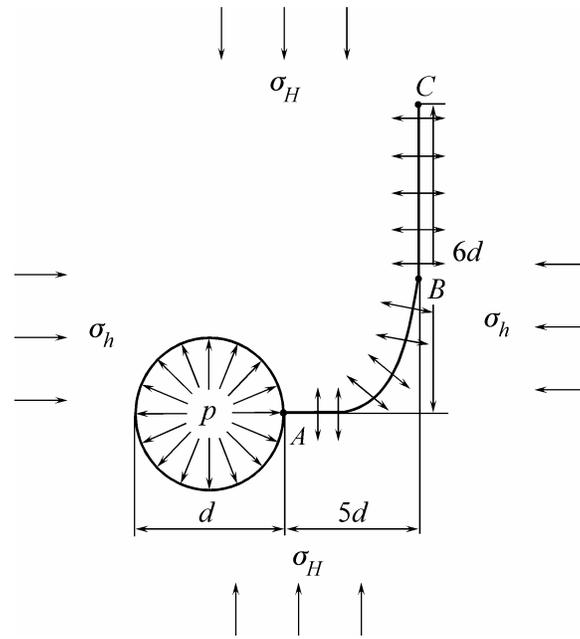
Fig. 3. Estimate for the role of digitizing the well contour and the "rear" portion of the hydraulic fracture

Let us compare three variants of the boundary element digitization of a fracture. The first variant: the well contour is divided into 24 arc elements (72 points of collocation, 144 real unknowns); first rectilinear segment with a length d is represented by 8 elements, the circle arc with a radius $4d$ and opening $\pi/4$ contains 30 elements; and, finally, a rectilinear segment BC with a length $2d$ is divided into 10 elements with the last one being a special end element. So, the total number of the elements is 72, the collocation points are $72 \cdot 3 = 216$, the real unknowns are $216 \cdot 2 = 432$.

The second variant: the well contour is divided into 4 elements; the rectilinear segment is one element, the contour arc is two elements, and the segment BC keeps division into 10 elements. As a result, only 7 elements instead of 62 remain for the well and the section AB. The total number for the second division variant elements is 17, the collocation points are $17 \cdot 3 = 51$; the real unknowns are $51 \cdot 2 = 102$, that is the unknowns are cut in number more than by a factor of four. The third variant differs from the second one by the well contour reduction into a rectilinear segment that, in principle, is a continuation of the fracture.

Eventually, we obtain the values of SIF at the front of the fracture (at the point C) and the fracture opening Δu_n. The rated K_I and Δu_n are found from the formulae:

$$\widetilde{K}_I = \frac{K_I}{\sigma_h \sqrt{\pi d/2}}; \quad |\Delta \widetilde{u}_n| = \frac{E}{\sigma_h} \frac{|\Delta u_n|}{d/2},$$

where E is Young's modulus of rocks.

For the three digitization variants above, the values of SIF are, respectively, 0.84, 0.80 and 0.91. Table 4 presents values of $|\Delta \widetilde{u}_n|$ at some characteristic points determined by the dimensionless coordinates x_1/d and x_2/d, where x_1 is counted from the marginal left-hand point of the well contour and x_2 is counted from the horizontal axis of symmetry of the well. The lines of Table 4 stand for the described variants.

50

TABLE 4. The Rated Displacement Discontinuities $\left|\Delta\widetilde{u}_n\right|$ at the Points of Trajectory for Three Digitization Variants for the Well and Fracture (Fig. 3)

Variant	x_1/d	1.50	3.53	5.69	6.00	6.00	6.00	6.00
	x_2/d	0.00	0.31	2.47	4.25	4.65	5.15	5.65
1		2.54	4.64	7.66	6.71	6.18	5.15	3.38
2	$\left\|\Delta\widetilde{u}_n\right\|$	2.60	4.45	7.07	6.03	5.72	4.85	3.22
3		2.37	4.64	8.66	7.64	6.95	5.72	3.72

Comparing the results shows that changing a fine element mesh into a coarse one in sections remote from the front causes a no more than 10 % difference in the calculated values (Table 4, lines 1 and 2). A supplementary change of the well contour circle by the rectilinear element with the length d (Table 4, line 3) produces much more difference: the deviation maximum is about 15 %.

We emphasize again that this example conforms to a rather nearby zone of the fracture propagation; this zone is of the order of $7-8d$, i.e., about 1 m. The farther is the fracture front from the well contour, the more accurate are the results of the presented above digitization techniques.

EXAMPLES AND ANALYSIS OF THE HYDRAULIC FRACTURE PROPAGATIONS

The Effect of the Initial Fracture Direction. Modeling results for two separate hydraulic fractures are shown in Fig. 4. The stress state components ratio $\sigma_H/\sigma_h = 2.0$. The initial fractures are at the angles of $0°$ and $60°$, respectively.

At the start stage of development (Fig. 4a), the trajectories differ greatly. Further growth almost in full aligns the difference (Fig. 4b). On the new scale, the fractures are parallel and are about $1.5d$ (approximately 0.2 m) apart from one the other, which makes them equivalent as far as their actual effect is concerned. By no means, in such examples, it is necessary to perform a thorough analysis of fractures that begin near the axes of symmetry, as a small difference in the onset conditions can entail strictly antipodal trajectories in this case.

The Developed Hydraulic Fracture SIF. Modeling a hydraulic fracture under a uniform stress state when such concentrators as the well or the geological disturbances have no effect, shows the following results [38, 39]. Irrespective initial orientation of the fracture relative to the directions of the principal stresses in a rock mass, only a short starting section of the trajectory can be curvilinear. After it, the fracture propagates towards the highest compressive stresses. This conclusions supports the earlier statements, for example, in [35].

The same fracturing pattern takes place for an isolated well. At a relatively small distance from the well $(3-5d$, Fig. 4a), that depends on the initial fracture orientation, the fracture develops along a curvilinear trajectory. Then this trajectory quickly tends to a straight line directed along the maximal compressive stresses. From the viewpoint of practice, in case there are no any disturbances or another well on the way of the fracture growth, we have that one of the main problems of modeling is solved: the fracture growth direction is determined.

Modeling a developed hydraulic fracture and a well as a straight line segment considerably simplifies both the SIF determination problem and the statement/answering of the question on estimating the permeability of fractures and the filtration parameters of enclosing rocks. In particular, it becomes possible to directly use the results of solving the problem on the rectilinear fracture with allowance for the fluid movement in the fracture and fluid filtration into the rock [35].
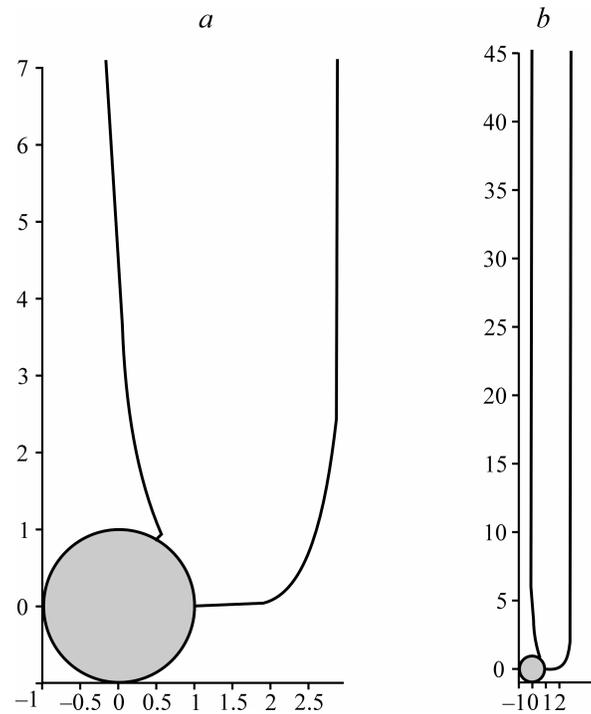
Fig. 4. Two phases of the hydraulic fracture propagation with initial fractures oriented at 0° and 60°:
a) the trajectory length is more than 3.5d; b) the trajectory length is more than 22.5d

Refer to the calculation data for K_I for the set of the hydraulic fracture trajectory points (Fig. 4, $\varphi = 60°$) as the fracture front moves away from the well. Table 5 presents SIF as a function of the coordinate x_2 of the current tip. The first line contains SIF by the BEM modeling, the second line cites SIF calculated from the formula:

$$K_I = (p - \sigma_h)\sqrt{\pi L / 2} \,, \tag{15}$$

where L is a length of the equivalent rectilinear fracture, $L = x_2 + d/2$. In the latter case, the fracture tip is assumed to be at a sufficiently large distance from the well so that the well effect is absent; that is, the equivalent fracture is under the joint action of the internal pressure and the stress σ_h applied at infinity. The values of SIF are rated similarly to Table 4, with taking into account that $\sigma_1^\infty = \sigma_h$.

The data from Table 5 indicate that when the hydraulic fracture is longer than 5d, the curvilinear part in the beginning of the trajectory and well looses its significance. Also, it should be noted that for a sufficiently extended hydraulic fracture, the dependence of K_I on the fracture length approaches a square root. Apropos fracture propagation condition (2), we see that, for satisfied (15) and large L, it is possible to assume that, at a high accuracy, the equality $p_s = \sigma_h$ holds true.

TABLE 5. Comparison of SIF for the Real and Equivalent Rectilinear Trajectory of a Hydraulic Fracture

x_2/d	1.21	2.39	3.58	4.86	6.05	7.75
$\widetilde{K}_I$	0.153	0.136	0.146	0.178	0.202	0.234
$\widetilde{K}_I$ eqv.	0.116	0.151	0.179	0.205	0.227	0.254

52

Bifurcation of the Trajectory. Allowing a reliable calculation of the trajectory for the alternating SIF K_I, the modified algorithm also assists in reproducing bifurcation of the trajectory when minor excitations can affect the choice of a fracture propagation path. The situation is such, for example, when the initial fracture is perpendicular to the direction of the maximum compression σ_H. In this case, in the initial position, we have $K_{II} = 0$ and condition (11) is met. The respective solution corresponds to the rectilinear propagation of fracture in its plane (in the perpendicular direction to σ_H). Nevertheless, when $\sigma_h < \sigma_H$, the trajectory is unstable, since the σ_h-perpendicular growth is more advantageous by ensuring a higher influx of energy. Therefore, a minor excitation of the rectilinear trajectory results in a curvilinear trajectory, more useful from the energy point of view. Actually, the excitation results from assigning a pre-introduced small start deviation of β^0 in iteration formulae (13), (14). As the calculation show, the modeled trajectory, according to physical concepts, quickly gets onto the direction that is perpendicular to the least compression σ_h. Note that the rectilinear trajectory bifurcation was studied earlier in the problems on tension of a plate with a crack [36, 38, 44, 48, 49], and it appears to be the first time when it is applied to the compression conditions.

Interference and Growth of Several Initial Fractures. The modeling method presented in the Introduction, encloses also the case when several initial fractures are at the well contour. The stress intensity factors can be calculated with taking into account the interference of the fractures and the well. We take the fracture with the highest SIF and trace its development after reaching the breakdown pressure values. The rest fractures, as a rule, will not propagate (we do not consider the case of the absolute symmetry when two or more fractures set on simultaneously), since the growth of one of them generally causes a decrease in K_I of the rest ones. The cases of the inverse effect are however possible to exemplify. One of them is the case when two fractures start from the well contour in almost diametrally opposite directions though close enough to the direction of the maximum compression (σ_h). At that time, the fracture with an angle closer to 90° or 270° begins growing. This growth must cause an increase in K_I for the second fracture, which provides for the limiting condition attainment and subsequent development of a new fracture. Analogous situations are probable when there are more initial fractures.

Another example is three fractures near a well, with angles of 80°, 258° and 284°, respectively. It is obvious that two of them are almost dissymmetrical relative to the coordinate origin. For the original principal stresses ratio $\sigma_H/\sigma_h = 1.5$ and the same length $l_0 = 0.1d$ of the three fractures, the calculation shows that the fracture with the angle $\varphi = 80°$ starts first. The breakdown pressure is $p_b = 1.0\sigma_h$ in this case and almost coincides with the breakdown pressure of a single initial fracture with $\varphi = 80°$, the other conditions the same. An insignificant growth of the other two fractures is noted at the same pressure. Then, we need a higher pressure $p = 1.05\sigma_h$ in order that the second fracture ($\varphi = 258°$) grows by d. Later, at this pressure sustained, the first fracture will intensively develop, then the first and the second fractures will grow, whereas the third fracture ($\varphi = 284°$) will remain fixed. The last development phase of the fractures is depicted in Fig. 5.

CONCLUSION

The article develops an approach to modeling a hydraulic fracture, based on the application of the up-to-date efficient computational technique, the boundary element method. The investigation results have been obtained for the initial stage of the hydraulic fracture propagation after reaching the breakdown pressure and for the extended fracture with its front tens meters away from the well.
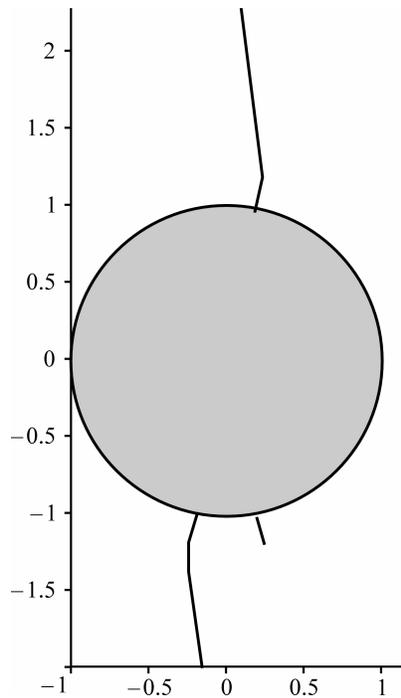
Fig. 5. Trajectories for three hydraulic fractures coming out of the same well, at the initial fracture angles of 80°, 258° and 284°

The results yield estimates for the important indices, such as breakdown pressure and fracture growth direction. Together with these, the study conditions a possibility for significant simplifications to be made in geometry of the scheme: a transfer to an analysis of a rectilinear fracture, which is of concern for a procedure of further investigations into the hydraulic fracturing.

We suppose the next research stage as 3-D modeling of the hydraulic fracture propagation. Additional characteristics connected with an instability of the fluid flow, friction effects and change in filtration properties of rocks should provide an advance in studying the hydraulic fracture development in time and in modeling the related seismic impulses.

The authors express their gratitude to A. M. Vaisman as a reviewer, for advising to include into the consideration the important and interesting works of colleagues, that were left out of eyeshot of the authors.

REFERENCES

1. Yu. P. Zheltov and S. A. Khristianovich, "On the hydraulic fracturing of an oil bed," *Izv. AN SSSR, OTN*, No. 5 (1955).
2. B. C. Haimson and C. Fairhurst, "Initiation and extension of hydraulic fractures in rocks," *Soc. Petrol. Eng. J.*, **7** (1967).
3. J. Geertsma and R. Haafkens, "A comparison of the theories predicting width and extent of vertical hydraulically induced fractures," *J. Energy Reservoir Technology*, **101** (1979).
4. K. G. Nolte and M. B. Smith, "Interpretation of fracturing pressures," *J. Petrol. Technol.*, Sept. (1981).
5. S. Nemat-Nasser, "Hydraulic fracturing and geothermal energy," *CIP* (1983).
6. N. R. Warpinski, "Measurement of width and pressure in a propagating hydraulic fracture," *Soc. Petrol. Eng. J.*, Feb. (1985).

7. M. P. Cleary, D. T. Barr, and R. M. Willis, "Enhancement of real-time hydraulic fracturing models with full 3-D simulator," in: *SPE Gas Technology Symposium*, Dallas, TX (1988).

8. L. L. Lacy, "Comparison of hydraulic fracture orientation techniques," *SPE Production & Facilities*, **2** (1987).

9. R. J. Pine and D. A. C. Nicol, "Analytical and numerical modeling of high pressure fluid-rock mechanical interaction in HDR geothermal energy reservoirs," in: *Comprehensive Rock Engineering: Principles*, *Practice&Projects*, J. Hudson (Ed.), **5** (1993).

10. F. Guo, J. R. Morgenstern, and J. D. Scott, "Interpretation of hydraulic fracturing breakdown pressure," *Int. J. Rock Mech.*, **30**, No. 6 (1993).

11. C. Atkinson and M. Thiercelin, "The interaction between the wellbore and pressure-induced fractures," *Int. J. Fracture*, **59** (1993).

12. S. A. Holditch, "Developing data sets for 3D fracture propagation models," *SPE Production & Facilities*, **9**, No. 4 (1994).

13. C. Atkinson and M. Thiercelin, "Pressurization of a fractured wellbore," *Int. J. Fracture*, **83** (1997).

14. L. Raymond, et al., "Improving results of coalbed methane development strategies by integrating geomechanics and hydraulic fracturing technologies," *SPE Asia Pacific Oil and Gas Conference and Exhibition*, Melbourne, Australia (2002).

15. R. W. Veatch, Jr., "Overview of current hydraulic fracturing design and treatment technology. Part 2," *Journal of Petroleum Technology*, May (1983).

16. M. M. Hossain, et al., "Hydraulic fracture initiation and propagation: roles of wellbore trajectory, perforation and stress regimes," *J. Petrol. Eng.*, **27** (2000).

17. M. M. Rahman, et al., "An integrated model multiobjective design optimization of hydraulic fracturing," *J. Petrol. Eng.*, **31** (2001).

18. V. N. Odintsev, "Theoretical estimate of influence exerted by borehole on the permeability of gas-saturated seam," *Fiz.-Tekh. Probl. Razrab. Polezn. Iskop.*, No. 6 (2001).

19. S. V. Slastunov, G. G. Karkashadze, and K. S. Kolikov, "Analytical model for hydraulic disjointing of coal seam," *Fiz.-Tekh. Probl. Razrab. Polezn. Iskop.*, No. 6 (2001).

20. A. G. Olovyanny, "Analytical model for hydraulic disjointing of coal seam," *Fiz.-Tekh. Probl. Razrab. Polezn. Iskop.*, No. 1 (2005).

21. A. A. Nasedkina and V. N. Trufanov, "Numerical modeling of hydrofracturing in a multilayer coal seam," *Fiz.-Tekh. Probl. Razrab. Polezn. Iskop.*, No. 1 (2006).

22. Yu. P. Zheltov, *Mechanics of the Oil-and-Gas-bearing Reservoir* [in Russian], Nedra, Moscow (1975).

23. C. Fairhurst, "Stress estimation in rock: a brief history and review," *Int. J. Rock Mechanics and Mining Sci.*, **40** (2003).

24. J. L. Gidley, et al. (Eds.), "Recent advances in hydraulic fracturing," *SPE Monograph* (1989).

25. B. C. Haimson and F. H. Cornet, "ISRM suggested methods for rock stress estimation. Part 3: Hydraulic fracturing (HF) and/or hydraulic testing of pre-existing fractures (HTPF)," *Int. J. Rock Mechanics and Mining Sci.*, **40** (2003).

26. L. S. Kolodko and P. A. Martynyuk, "On development and coalescence of two pre-parallel rectilinear cracks," *Fiz.-Tekh. Probl. Razrab. Polezn. Iskop.*, No. 4 (1989).

27. T. E. Alekseeva and P. A. Martynyuk, "Crack emergence trajectories at a free surface," *Fiz.-Tekh. Probl. Razrab. Polezn. Iskop.*, No. 2 (1991).

28. P. A. Martynyuk and E. N. Sher, "Development of a crack close to a circular opening with an external field of compressive stresses," *Fiz.-Tekh. Probl. Razrab. Polezn. Iskop.*, No. 6 (1996).

29. P. A. Martynyuk, "Trajectory of crack formed by hydraulic fracturing near the contact of productive stratum with enclosing rocks," *Fiz.-Tekh. Probl. Razrab. Polezn. Iskop.*, No. 4 (2002).

30. E. N. Mastrojannis, L. Keer, and T. Mura, "Growth of planar cracks induced by hydraulic," *Int. J. Num. Meth. Eng.*, **15** (1980).

31. D. A. Mendelsohn, "A review of hydraulic fracture modeling. Part I: General concepts, 2D models, motivation for 3D modeling," *J. Energy Res. Tech.*, **106** (1984).

32. S. Mogilevskaya, et al., "Growth of pressure-induced fractures in the vicinity of a wellbore," *Int. J. Fracture*, **104** (2000).

33. V. Koshelev and A. Ghassemi, "Numerical modeling of stress distribution and crack trajectory near a fault or a natural fracture," in: *Soil and Rock America 2003; 30th US Rock Mechanics Symposium*, Cambridge, Mass. Eds.: P. J.Culligan, et al. (2003).

34. V. Koshelev and A. Ghassemi, "Hydraulic fracture propagation near a natural discontinuity," in: *Proceedings of the 28th Workshop on Geothermal Reservoir Engineering*, Stanford University, Stanford, California (2003).

35. O. P. Alekseenko and A. M. Vaisman, "Certain aspects of a two-dimensional problem on the hydraulic fracturing of an elastic medium," *Fiz.-Tekh. Probl. Razrab. Polezn. Iskop.*, No. 3 (1999).

36. M. P. Savruk, *2D Elasticity Problems for Bodies with Cracks* [in Russian], Naukova Dumka, Kiev (1981).

37. A. M. Lin'kov, *Complex Method of Boundary Integral Equations of Elasticity Theory* [in Russian], Nauka, Saint Petersburg (1999).

38. A. A. Dobroskok, "Numerical modeling of the constitutive relations for a medium with cracks and contact interactions," *Doctoral Thesis* [in Russian], IPMash, Saint Petersburg (2002).

39. A. Dobroskok, "On a new method for iterative calculation of crack trajectory," *Int. J. Fracture*, **111** (2001).

40. E. Detournay and R. Carbonell, "Fracture mechanics analysis of the breakdown process in minifrac or leak-off tests," in: *Proceedings EUROCK 94 Symposium*, Delft (1994).

41. U. Mourakami (Ed.), *Stress Intensity Factors. Guide* [Russian translation], **1**, Mir, Moscow (1985).

42. N. M. Osipenko, "Studying the mechanism of brittle fracture in jointy rocks," *Candidate's Thesis* [in Russian], IFZ AN SSSR, Moscow (1972).

43. V. N. Nikolaevskii, "Review: Earth crust, dilatancy and earthquakes," in: *Mechanics of the Earthquake Focus* [Russian translation], J. Rice (Ed.), Mir, Moscow (1982).

44. R. Cotterell and J. R. Rice, "Slightly curved or kinked cracks," *Int. J. Fracture*, **16**, No. 2 (1980).

45. A. M. Lin'kov and A. A. Dobroskok, "Numerical modeling of rock deformation under compression," *Fiz.-Tekh. Probl. Razrab. Polezn. Iskop.*, No. 4 (2001).

46. A. A. Dobroskok, A. M. Linkov, L. Myer, and J.-C. Roegiers, "On a new approach in micromechanics of solids and rocks," in: *Rock Mechanics in the National Interest, Proceedings of the 38th US Rock Mechanics Symposium*, Tinucci & Heasley (Eds), Swets&Zeitlinger Lisse (2001).

47. A. A. Dobroskok, A. Ghassemi, and A. M. Linkov, "Extended structural criterion for numerical simulation of crack propagation under compressive loads," *Int. J. Fracture*, **133** (2005).

48. J. C. Radon, P. S. Leevers, and L. E. Culver, "Fracture toughness of PMMA under biaxial stress," *Fracture*, **8** (1977).

49. S. G. Mogilevskaya, "Numerical modeling of 2D smooth crack growth," *Int. J. Fracture*, **87** (1997).